

## **Supporting Information**

# **Real-time dynamic SERS Galectin detection using glycan-decorated gold nanoparticles**

Judith Langer,<sup>a,b</sup> Isabel García<sup>a,b</sup> and Luis M. Liz-Marzán<sup>a,b,c</sup>

<sup>1</sup> CIC biomaGUNE, Paseo de Miramón 182, 20014 Donostia-San Sebastián, Spain.

<sup>2</sup>Biomedical Research Networking Centre on Bioengineering, Biomaterials and Nanomedicine  
(CIBER-BBN), *Paseo Miramón 182*, 20014 Donostia, San Sebastián, Spain.

<sup>3</sup>Ikerbasque, Basque Foundation for Science, 48011 Bilbao, Spain.

## Characterization of SERS nanotags

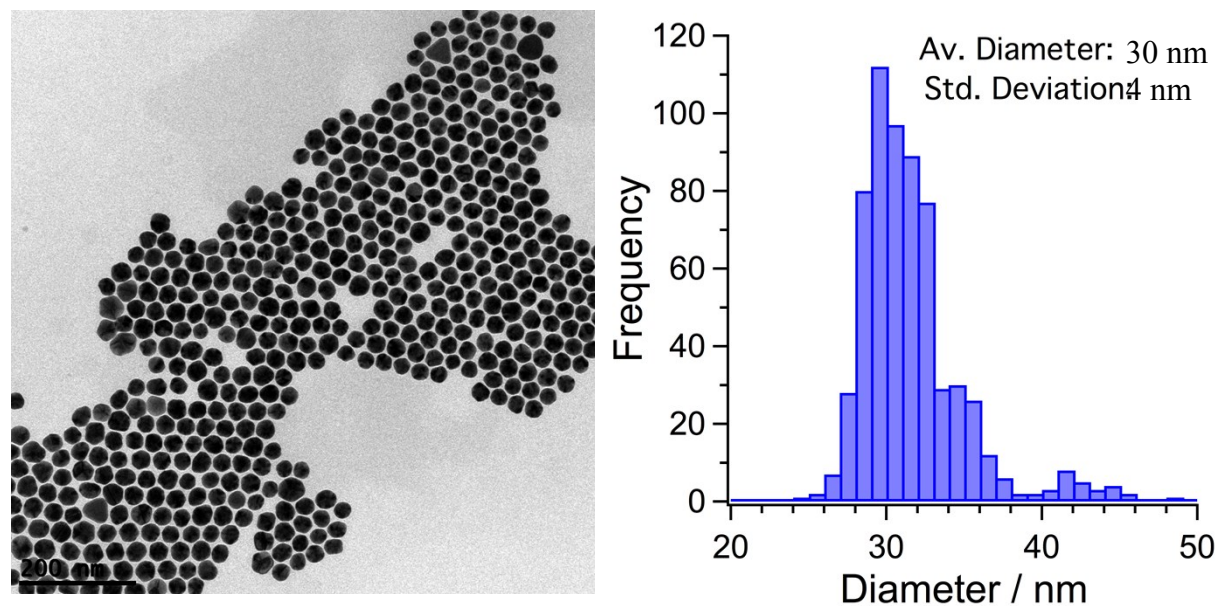


**Fig. S1** Representative TEM images and size distribution of glycan-decorated 4-MBA-modified Au NPs (SERS nanotags). The average diameter was 29.9 nm, with a standard deviation of 4.0 nm.

## Analysis of the Au NPs surface functionalization with thiolated glycan and 4-MBA

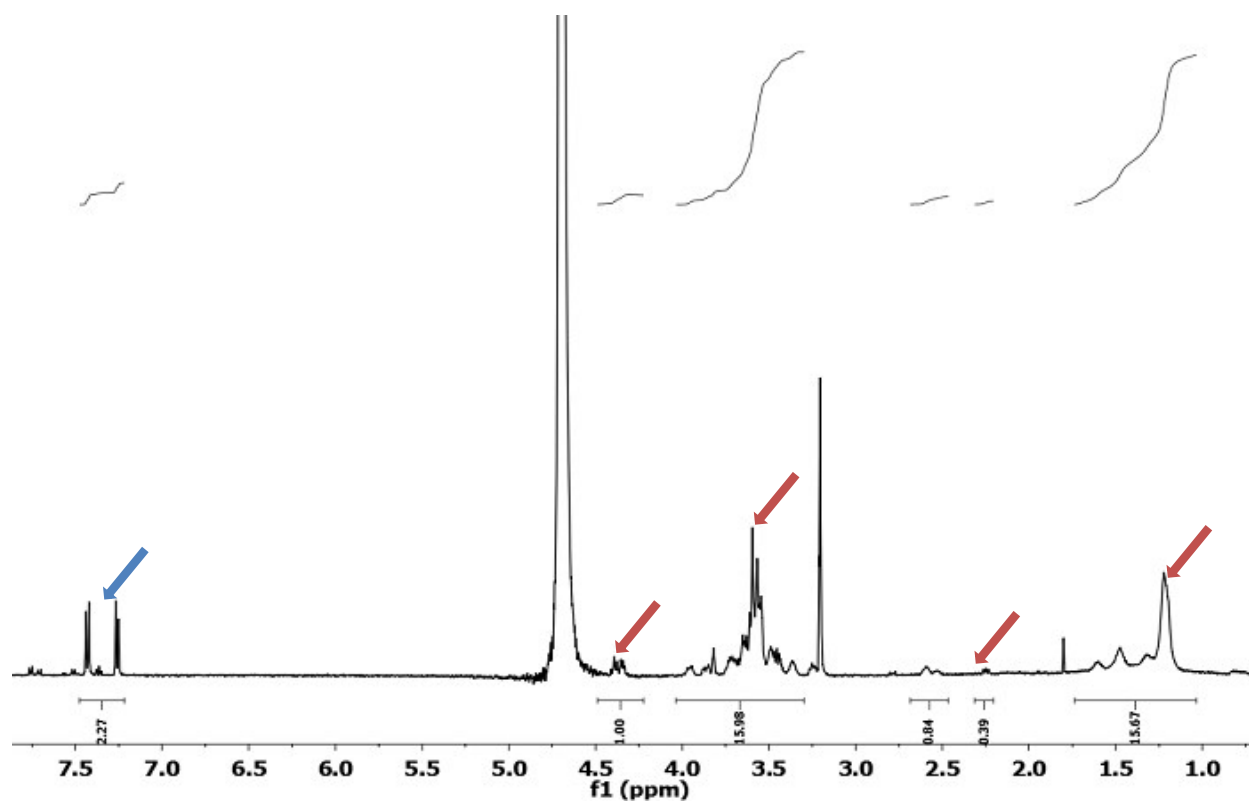


**Fig. S2** <sup>1</sup>H-NMR spectrum of SERS nanotags registered after treatment with cyanide. The red arrows indicate signals assigned to glyconjugates and the blue narrows indicate signals attributed to residual 4-MBA molecules.

## Gal-9 SERS sensing

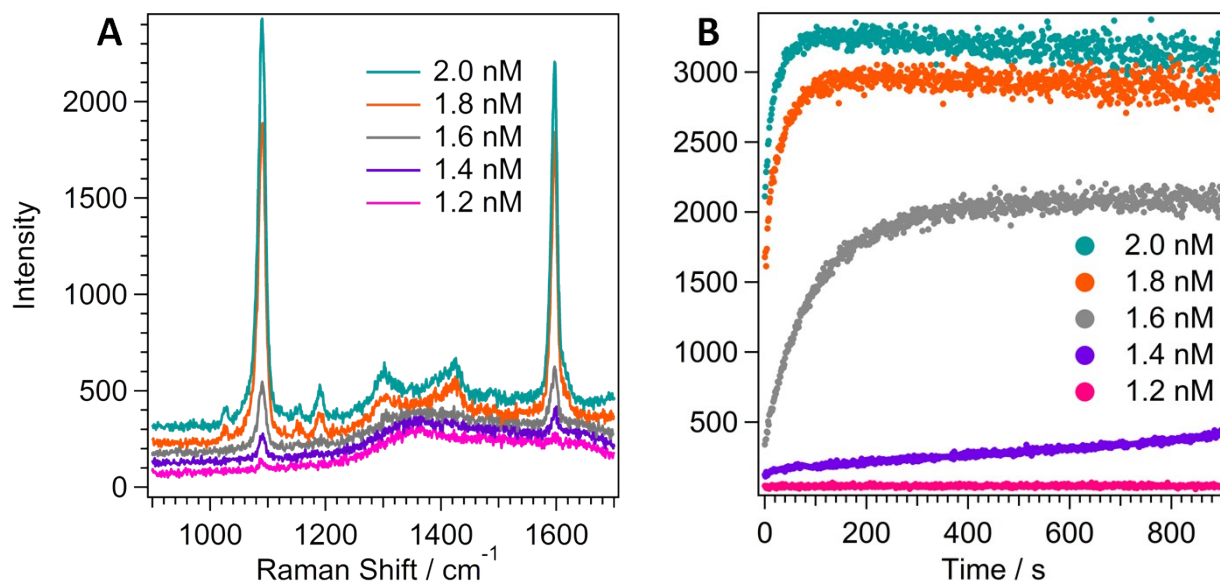


**Fig. S3** (A) SERS spectra from Gal-9-driven aggregation of SERS nanotags, under 20:1 mixing volume conditions, for different Gal-9 concentrations, recorded at  $t=0$  (immediately after incubation), with integration time of 1s and laser power of 45mW. Spectra were not baseline corrected and plotted with offsets of 50 (1.4 nM), 100 (1.6 nM), 150 (1.8 nM) and 200 cps (2.0 nM) for more convenient data representation. (B) Time-dependent SERS intensities ( $1078\text{ cm}^{-1}$ ) for the same samples showing the different aggregation kinetics, depending on the Gal-9 concentration. SERS kinetic profiles of 2.0, 1.8 and 1.6 nM reveal a fast cluster growth in the early time window with linear SERS response, which becomes slower until a plateau is reached. The continuously rising SERS signal at 1.4 nM Gal-9 concentration indicates slow aggregation, whereas not progressive aggregation is observed at 1.2 nM, due to the low aggregation rate within the presented observation time window.

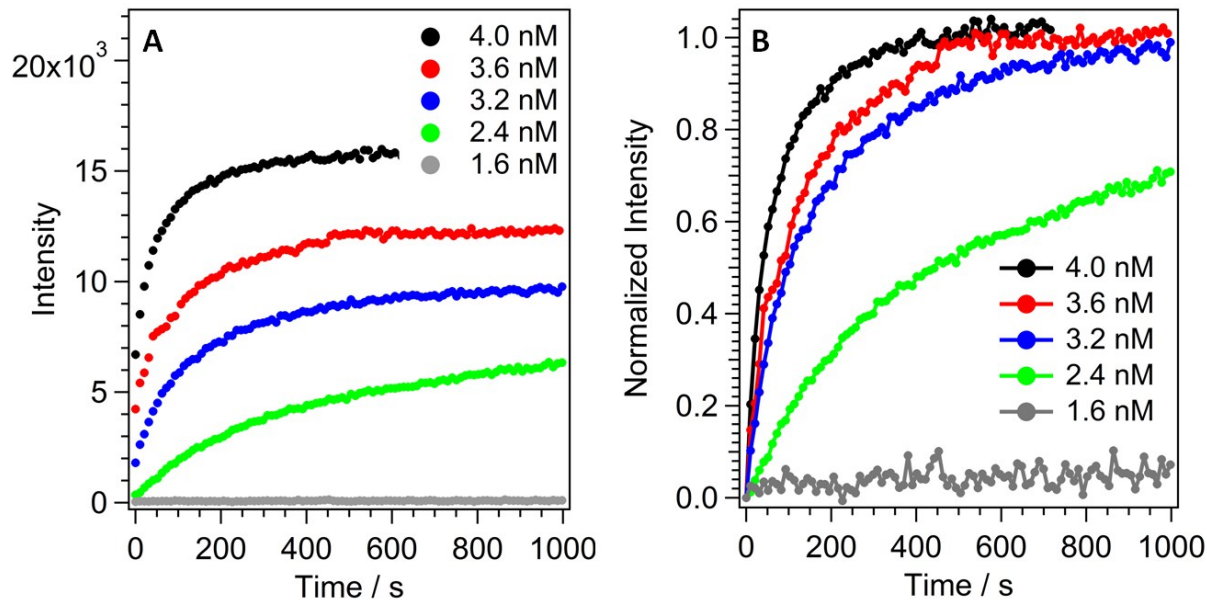


**Fig. S4** (A) Time-resolved SERS signals of Gal-9-driven SERS nanotag aggregation under 1:1 mixing volume conditions, showing that the plateau is reached at longer time scales and the SERS intensity of the plateau decreases with decreasing Gal-9 concentration, indicating slower aggregation and leading to smaller cluster sizes. (B) Normalization of the SERS intensities shows the differences in aggregation dynamics depending on Gal-9 concentration. With decreasing Gal-9 concentration, the duration of the linear stage becomes longer and the slope of linear part becomes shorter due to significantly slower cluster growth. The aggregation dynamics at 1.6 nM are too slow to be detected within the presented observation time window.

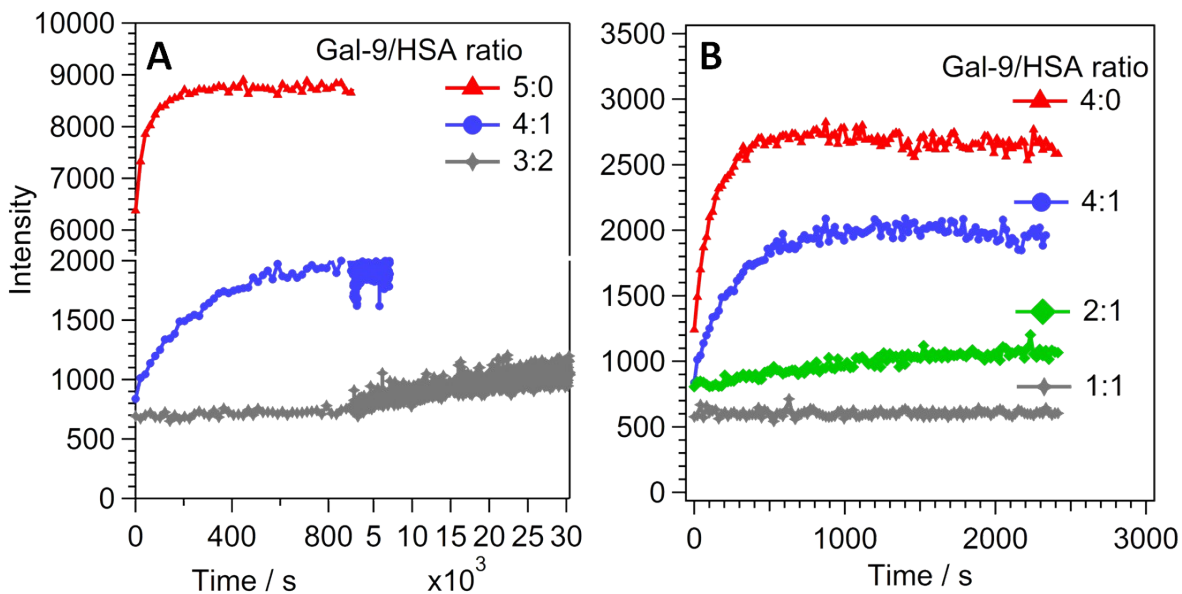


**Fig. S5** (A) Time-resolved SERS signal ( $1078\text{ cm}^{-1}$ ) of Gal-9-driven SERS nanotag aggregation under 20:1 mixing volume conditions, in coexistence of different molar fractions of non-specifically binding protein HSA, for constant total protein concentration (Gal-9+HSA). The ratio of 5:0 corresponds to 2.0 nM Gal-9 final concentration, 4:1 to 1.6 nM Gal-9 and 0.4 nM HSA final concentrations and 3:2 to 1.2 nM Gal-9 and 0.8 nM HSA final concentrations. The time axis is amplified between 0-900s and the y-axis is sliced and cut between 2000-5000 for better representation. (B) Time-resolved SERS signal ( $1078\text{ cm}^{-1}$ ) of Gal-9-driven SERS nanotag aggregation under 20:1 mixing volume conditions in coexistence of different molar fractions of the non-specifically binding protein HSA for 1.6 nM Gal-9 final concentration. The ratio of 4:0 corresponds to solution without HSA, 4:1 to 0.4 nM HSA final concentration, and 2:1 to 0.8 nM HSA final concentration, 1:1 to 1.6 nM HSA final concentration. Note that total protein concentration increases from 1.6 nM to 3.6 nM. The SERS profiles of A and B show that the recognition of Gal-9 is significantly hindered when HSA concentration are increased, leading to lower aggregation rates and formation of smaller clusters, but still detectable SERS signals.